Aging Cell (2013) **12**, pp214–223 Doi: 10.1111/acel.12043

Quantification of *in vivo* oxidative damage in *Caenorhabditis elegans* during aging by endogenous F3-isoprostane measurement

Christiaan F. Labuschagne,[1] Edwin C. A. Stigter,[1] Margriet M. W. B. Hendriks,[1] Ruud Berger,[1] Joshua Rokach,[2] Hendrik C. Korswagen[3] and Arjan B. Brenkman[1]

[1]University Medical Center Utrecht, Department of Metabolic Diseases and Netherlands Metabolomics Center, Utrecht, 3508 AB, The Netherlands
[2]Claude Pepper Institute and Department of Chemistry, Florida Institute of Technology, Melbourne, FL, 32901, USA
[3]Hubrecht Institute, Royal Academy of Arts and Sciences and University Medical Center Utrecht, Utrecht, 3508 AD, The Netherlands

Summary

Oxidative damage is thought to be a major cause in development of pathologies and aging. However, quantification of oxidative damage is methodologically difficult. Here, we present a robust liquid chromatography–tandem mass spectrometry (LC-MS/MS) approach for accurate, sensitive, and linear *in vivo* quantification of endogenous oxidative damage in the nematode *Caenorhabditis elegans,* based on F3-isoprostanes. F3-isoprostanes are prostaglandin-like markers of oxidative damage derived from lipid peroxidation by Reactive Oxygen Species (ROS). Oxidative damage was quantified in whole animals and in multiple cellular compartments, including mitochondria and peroxisomes. Mutants of the mitochondrial electron transport proteins *mev-1* and *clk-1* showed increased oxidative damage levels. Furthermore, analysis of Superoxide Dismutase (*sod*) and Catalase (*ctl*) mutants uncovered that oxidative damage levels cannot be inferred from the phenotype of resistance to pro-oxidants alone and revealed high oxidative damage in a small group of chemosensory neurons. Longitudinal analysis of aging nematodes revealed that oxidative damage increased specifically with postreproductive age. Remarkably, aging of the stress-resistant and long-lived *daf-2* insulin/IGF-1 receptor mutant involved distinct *daf-16*-dependent phases of oxidative damage including a temporal increase at young adulthood. These observations are consistent with a hormetic response to ROS.

Key words: aging; *C. elegans*; F3-isoprostanes; Insulin/IGF-1; mitohormesis; oxidative damage; ROS; SOD.

Introduction

The universal phenomenon of aging is a complicated biological process with a mechanism that lacks overall understanding. The nematode *C. elegans* served as a paradigm in the field of aging ever since the discovery that single-gene mutations or environmental manipulations could double its lifespan (Kenyon, 2010). For instance, mutations in the insulin/IGF-1 receptor *daf-2* were found to extend lifespan up to threefold, a process that is completely suppressed by the Forkhead transcription factor *daf-16* (Kenyon, 2010). The insulin/IGF-1 pathway and its role in longevity are highly conserved and a remarkable hallmark of these and other longevity mutants is a phenotype of increased resistance to cellular stress, including oxidative stress (Kenyon, 2010). These findings are consistent with the Free Radical Theory of Aging, which was formulated back in 1956 and explains aging through accumulation of oxidative damage to macromolecules (Harman, 1956).

To minimize damage from ROS, stress protective response pathways have evolved. These are highly conserved and consist of complex systems of both defense and sensing mechanisms, which include superoxide dismutase (SOD), catalase (Ctl), peroxiredoxins, and glutathione peroxidase enzymes (Halliwell, 1999). SODs scavenge the highly reactive and local superoxide ($O_2^{-}\bullet$) radicals and dismutate them to hydrogen peroxide (H_2O_2). H_2O_2 can readily cross membranes and in turn is further reduced by catalase, peroxiredoxins and glutathione peroxidase. In the presence of transition metal ions, hydrogen peroxide can be converted via a Fenton reaction to another highly reactive radical, $OH^{\bullet}$. In addition to the generation of damage, ROS have been shown to play a critical role in signaling as well and the balance between signaling and damage is a field of intense research.

A major obstacle, however, in understanding the contribution of ROS in the generation of oxidative damage or signaling in *C. elegans* in aging is the widely recognized methodological difficulties to measure ROS and its derived oxidative damage *in vivo* in living organisms (Van Raamsdonk *et al.*, 2010; Muller *et al.*, 2007; Gems & Doonan, 2009). Instead, the role of oxidative damage has therefore often been inferred through indirect assays, including resistance to pro-oxidants, knockout or transgenic analysis of ROS scavenging enzymes and respiration assays, each with their own pitfalls (Muller *et al.*, 2007). As production of oxidative damage depends both on the levels of ROS and the scavenging capacity of the organism, there is a clear need for methods to directly quantify oxidative damage and ROS. Through design of unique fluorescent probes, recent studies quantified H_2O_2 and established the glutathione redox state in *C. elegans* (Back *et al.*, 2012) and *Drosophila* (Albrecht *et al.*, 2011) *in vivo*. Moreover, another study reported a mitochondrial targeted probe quantified by ratiometric mass spectrometry to measure H_2O_2 in mitochondria in living *Drosophila*, which illustrates the potential use of mass spectrometry toward quantification of ROS in signaling (Cocheme *et al.*, 2011). Although these studies enable ROS measurements, methods to accurately determine endogenous oxidative damage in *C. elegans* are lacking.

Correspondence
Arjan B. Brenkman, University Medical Centre Utrecht, Department of Metabolic Diseases and Netherlands Metabolomics Centre, Lundlaan 6, 3508 AB, Utrecht, The Netherlands, Tel.: +31-8875-54921; fax: +31-8875-4295, e-mail: a.b.brenkman@umcutrecht.nl

Accepted for publication *18 December 2012*

The predominant mammalian poly-unsaturated fatty acid (PUFA), arachidonic acid (AA, C20:4, ω3), can give rise to F2-isoprostanes through extraction of an electron on one of the four double bonds by both superoxide and hydroxyl radicals (Morrow *et al.*, 1990; Rokach *et al.*, 1997; Pratico *et al.*, 2004). Because of their chemical stability, these nonenzymatic lipid peroxidation products are regarded as the gold standard for oxidative damage quantification in mammalian plasma and urine (Pratico *et al.*, 1998; Kadiiska *et al.*, 2005). Furthermore, F3-isoprostanes derived from another PUFA, Eicosapentaenoic acid (EPA), were also recently identified as markers for oxidative damage in mammals (Gao *et al.*, 2006; Chang *et al.*, 2008; Song *et al.*, 2009). Here, we present an approach for *in vivo* quantification of endogenous oxidative damage in *C. elegans* through a mass spectrometry-based stable isotope dilution assay of F3-isoprostanes. The method is characterized as highly specific, sensitive, accurate, and linear over a wide dynamic range and it enabled for the first time absolute quantification of endogenous levels of oxidative damage in *C. elegans in vivo*. We validated it on *C. elegans* strains knockout or transgenic for ROS scavenging *sod* and *ctl* genes which showed an expected increase in F3-isoprostanes levels at young adulthood as compared with wild-type for most, but not all mutants. Levels of oxidative damage could be assessed and quantified in the cytoplasm, mitochondria, and peroxisomes as well as in a small set of chemosensory neurons specifically. Unexpectedly, whereas mutants of *sod-1*, encoding the predominant cytoplasmic SOD, showed exceptional sensitivity to the pro-oxidant paraquat (PQ), the levels of oxidative damage at steady state were wild-type-like, underscoring the need to directly quantify oxidative damage *in vivo*. Moreover, mitochondrial *clk-1* and *mev-1* mutants which are affected in electron transport chain activity showed increased oxidative damage levels. Oxidative damage increased exponentially in the aging worm starting from the postreproductive phase. Surprisingly, we found that the long-lived *daf-2* mutant has strongly increased *daf-16* dependent levels of oxidative damage as compared with wild-type controls in young adulthood. However, these levels abated postreproductively and were significantly lower during aging than wild-type nematodes in a *daf-16*-dependent manner. These findings have important implications for how oxidative damage may contribute to aging.

Results

F3-isoprostanes are produced from EPA in the nematode *C. elegans*

To identify isoprostanes in *C. elegans,* we searched for the presence of AA and other PUFA's. In contrast with mammals, we found EPA (C20:5, ω3) to be the predominant *C. elegans* PUFA (Fig. S1A) in agreement with previous reports (Watts & Browse, 2002). As noted above, EPA contains five double bonds and has recently been shown to give rise to F3-isoprostanes in response to *in vivo* oxidative damage (Gao *et al.*, 2006; Chang *et al.*, 2008). These observations initiated our search for the presence of F3-isoprostanes as markers of lipid peroxidation in *C. elegans*. Comparison of chromatograms of *C. elegans* homogenates to that of copper-induced *in vitro* oxidized esterified EPA, showed high similarity with corresponding multiple reaction monitoring (MRM) peaks at different retention times which may represent different F3-isoprostane isomers (Fig. 1A). Using tetradeuterated standards of two recently characterized F3-isoprostanes (Chang *et al.*, 2008), which have the same chemical properties as endogenous F3-isoprostanes but with a higher *m/z* value, two of the endogenous peaks in the *C. elegans* homogenate were identified as 5-epi-8,12-iso-iPF3α-VI, and 8,12-iso-iPF3α-VI (Fig. 1B), suggesting that *C. elegans* contains at least two F3-isoprostane isomers [an alternative isoprostane nomenclature is also in use (Taber *et al.*, 1997)]. The identity was confirmed by collision-induced dissociation (CID) mass spectral analysis of labeled and unlabeled F3-isoprostanes (Fig. S1B) and by coinjection of pure synthesized standards (Fig. S1C). To demonstrate that F3-isoprostanes are indeed formed from oxidation of EPA, we subjected eicosapentaenoyl PAF-C16, an EPA-containing glyceryl-3-phosphorylcholine, to *in vitro* lipid peroxidation and monitored the formation of F3-isoprostanes in time (Fig. 1C). Lipid peroxidation by Cu^{++} is a simple and reproducible *in vitro* model for studying oxidative damage to lipids (Maiorino *et al.*, 1995). The mechanism of copper-induced lipid peroxidation is proposed to be as follows: $LOOH + Cu^{++} \rightarrow LOO^{\bullet} + Cu^{+}$ or $LOOH + Cu^{+} \rightarrow LO^{\bullet} + Cu^{++}$.

The fatty acid peroxyl radicals ($LOO^{\bullet}$) that are formed initiate a chain reaction of lipid peroxidation that results in the formation of chemically stable lipid peroxidation end products (Chamulitrat & Mason, 1989). As expected, F3-isoprostane levels increased in a time-dependent manner (Fig. 1C). To confirm that the F3-isoprostane formation results from oxidation, the antioxidant butylated hydroxytolueen (BHT) was added, which converts peroxyl radicals to hydroperoxides (LOOH) and subsequently terminates the chain reaction. Indeed, F3-isoprostane formation was inhibited by BHT (Fig. 1C). Incubation of *C. elegans* homogenate with Cu^{++} also induced lipid peroxidation which was blunted by both BHT and Trolox, a vitamin E-derived antioxidant (Fig. 1D). Thus, F3-isoprostanes can indeed be formed as nonenzymatic lipid peroxidation products in *C. elegans* homogenates and can be used as markers for oxidative damage. Furthermore, as shown in Fig. S2 and Table S1, this isotope dilution method is highly linear, sensitive, accurate, and precise and can be used for absolute F3-isoprostane quantification (for a detailed method description see Supplementary information).

F3-isoprostanes as *in vivo* markers of oxidative damage in *C. elegans*

Because of the lack of sensitive methods to measure *in vivo* oxidative damage in *C. elegans*, PQ survival is often used as a readout for sensitivity to oxidative damage (Van Raamsdonk & Hekimi, 2009). PQ undergoes a redox cycling reaction *in vivo* by accepting a single electron from NADPH after which the electron is donated to molecular oxygen resulting in the formation of $O_2^{-}\bullet$, the primary ROS species in the cell (Krall *et al.*, 1988). We subjected young adult N2 worms to a 200-mM PQ solution and compared the F3-isoprostane levels over time with untreated controls (Fig. 2A, left panel). In parallel, the same experiment was performed on a smaller

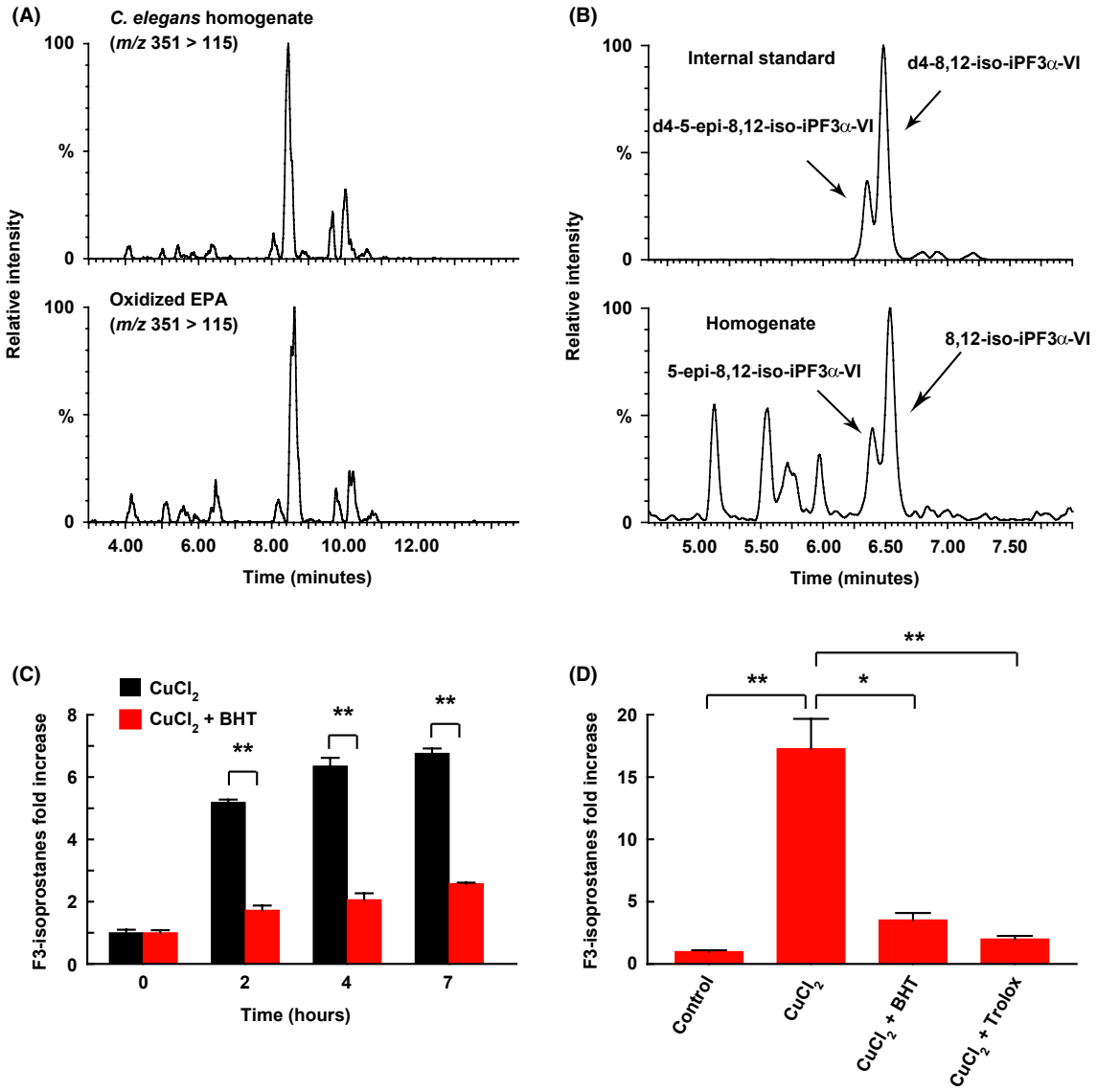

Fig. 1 Identification of two F3-isoprostane isomers in *C. elegans*. (A) EPA oxidation products are identified in a *C. elegans* homogenate by LC-MS/MS. Representative MRM chromatograms show peaks corresponding to F3-isoprostanes (*m/z* 351 > 115) in *C. elegans* homogenate (top panel) and in an esterified EPA (EPA-PAF-C16) standard, oxidized with $CuCl_2$ (bottom panel). (B) Deuterated F3-isoprostane isomer standards coelute with F3-isoprostane peaks in *C. elegans* homogenate. Chromatograms showing MRM of d4-labeled 5-epi-8,12-iso-iPF3α-VI, and 8,12-iso-iPF3α-VI (*m/z* 355 > 115) coeluting with endogenous peaks (*m/z* 351 > 115). (C) F3-isoprostanes were formed in a time-dependent manner by Cu^{++} -induced EPA *in vitro* peroxidation, which is quenched by the antioxidant BHT. EPA-PAF-C16 was incubated with 50-μM $CuCl_2$ for the indicated time points either in the presence or absence of BHT. (D) The antioxidants BHT and Trolox inhibited F3-isoprostane formation in a copper-treated *C. elegans* homogenate. A *C. elegans* homogenate was incubated with 50-μM $CuCl_2$ for 24 h either in the presence or absence of 100 μM BHT or 10-mM Trolox. The significance of changes in panels C and D was confirmed by Welch's *t*-test and are shown as mean ± SD. (**$P < 0.01$, *$P < 0.05$).

scale to monitor mortality (Fig. 2A, right panel). There is a clear time-dependent increase in F3-isoprostane production in response to PQ treatment as compared with untreated controls (Fig. 2A), confirming that PQ induced *in vivo* oxidative damage in *C. elegans*. An alternative protocol for exposure of nematodes to PQ is through supplementation on plate (Van Raamsdonk & Hekimi, 2009). A 4-mM PQ dose was sufficient to increase oxidative damage, which could be blunted through cosupplementation of trolox (Fig. 2B) further indicating that PQ induced *in vivo* oxidative damage. As biological effects of PQ have been reported using lower PQ concentrations (Yang & Hekimi, 2010), we next tested a PQ concentration range on plate and noted a significant increase in F3-isoprostanes after nematodes were exposed to low PQ concentrations of 0.05 mM (Fig. 2C). To determine the site of PQ-mediated oxidative damage production in the cell, we subjected two SOD mutant strains to a 50-mM PQ solution. *sod-1* is the predominant Cu/ZnSOD present in the cytoplasm, which when mutated reduces total SOD activity by 80% (Doonan *et al.*, 2008) whereas *sod-2* is the predominant mitochondrial MnSOD (Hunter *et al.*, 1997). Figure 2(D) shows a dramatic time-dependent F3-isoprostane

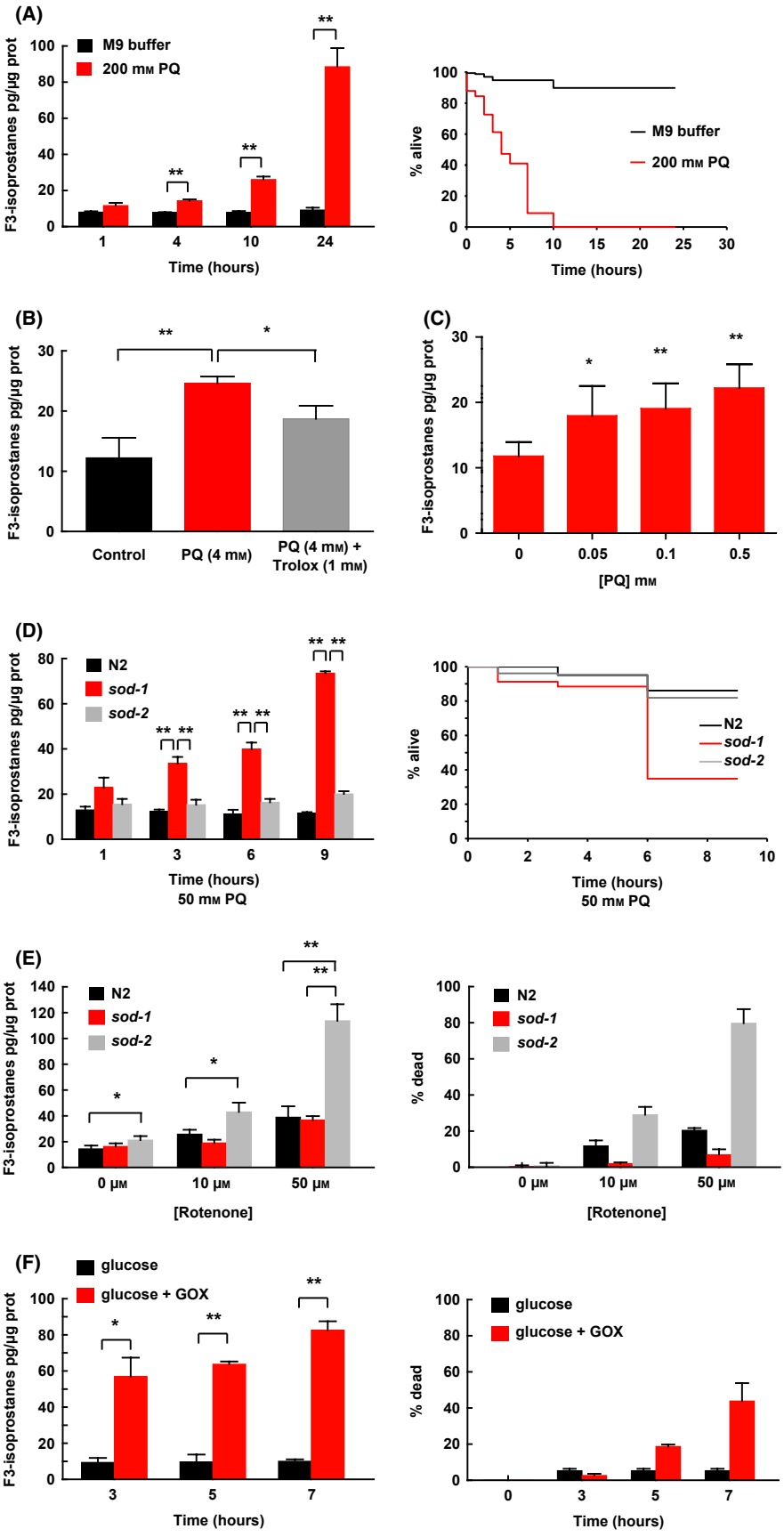

Fig. 2 F3-isoprostanes as *in vivo* markers of oxidative stress. (A) *In vivo* F3-isoprostane levels and death in *C. elegans* increased in a time-dependent manner in response to PQ treatment. N2 worms were treated in solution with 200-mM PQ for indicated times and analyzed for F3-isoprostanes by LC-MS/MS (left panel). In a parallel experiment, survival was monitored (right panel). (B) Oxidative damage induction by PQ is quenched by the antioxidant trolox. N2 nematodes were exposed to 4-mM PQ on plate either in the absence or presence of trolox for 3 days. (C) Exposure to low PQ concentrations induced F3-isoprostanes. N2 nematodes were exposed to indicate concentrations of PQ on plate for 3 days. (D) The *sod-1* mutant showed a specific increase in F3-isoprostane levels in response to 50-mM PQ. N2, *sod-1*, and *sod-2* worms were treated in solution with 50-mM PQ for indicated times and were analyzed for F3-isoprostanes (left panel). In a parallel experiment, survival was monitored (right panel). (E) Rotenone exposure predominantly induces F3-isoprostane formation in *sod-2* mutants. N2, *sod-1*, and *sod-2* worms were treated in solution with indicated concentration of rotenone for 24 h followed by F3-isoprostane analysis (left panel). Survival was scored in a parallel experiment (right panel). (F) Glucose oxidase (GOX) induces *in vivo* F3-isoprostanes in N2 worms. Worms were treated in solution with 50 mU GOX for indicated times and were analyzed for F3-isoprostanes (left panel). In a parallel experiment, survival was monitored (right panel). Data were expressed as means ± SD and significance was confirmed by Welch's *t*-test (***P* < 0.01, **P* < 0.05) for panels A, D–F and Student's *t*-test for panels B,C.

increase in the *sod-1* mutant as compared with *sod-2* and N2, suggesting that PQ-induced oxidative damage is at least formed in the cytoplasm.

Next, we examined if our developed method enables measurement of oxidative damage from ROS produced in the mitochondria, which are considered to be the main site for ROS production (Paraidathathu *et al.*, 1992). N2, *sod-1* and *sod-2* mutant strains were exposed to rotenone, a Complex I inhibitor of the mitochondrial electron transport chain which enhances mitochondrial ROS production (Li *et al.*, 2003). An increase in F3-isoprostanes was observed in all three strains (Fig. 2E). In contrast with PQ treatment, however, F3-isoprostanes were predominantly formed in the *sod-2* mutant, confirming that the site of ROS production by rotenone mainly occurs in the mitochondria. Next, we exposed N2 worms to an exogenous source of ROS in the form of H_2O_2, produced by the enzyme glucose oxidase (GOX). In the presence of D-glucose and oxygen, GOX catalyzes D-glucose oxidation into D-glucose-1,5-lactone and a constant flux of H_2O_2. After 3 h of GOX exposure, a sixfold induction of F3-isoprostane levels was measured which increased further to 8.5-fold induction after 7 h as compared with control worms (Fig. 2F). Thus, endogenous *in vivo* oxidative damage caused by ROS, produced at different cellular compartments in *C. elegans*, including the cytoplasm, mitochondria, and exogenously can be readily quantified using F3-isoprostanes.

Oxidative damage in ROS scavenging mutants, mitochondrial mutants, and during aging

H_2O_2 acts as an important signaling molecule that can diffuse over cell membranes to other compartments. To prevent hydroxyl radical formation by H_2O_2, *C. elegans* has three catalases which reduce H_2O_2 to water and oxygen. *ctl* genes are expressed at specific cellular locations, including the cytosol (*ctl-1)* and peroxisomes (*ctl-2),* whereas the location of *ctl-3* gene expression has not been reported. All three mutant strains showed increased *in vivo* oxidative damage as compared with N2 (Fig. 3A), indicating that oxidative damage originating from hydroxyl radicals produced in the cytoplasm and peroxisomes can be readily detected and quantified by this method. Moreover, it suggests that functional redundancy from other scavenging enzymes does not prevent an increase in oxidative damage. Conversely, transgenic expression of all three *ctl* genes in the *wuIs151*(*ctl-1* + *ctl-2* + *ctl-3* + myo-2::GFP) strain reduced oxidative damage levels to below wild-type levels (Fig. 3B).

In addition to the major cytoplasmic Cu/ZnSOD and mitochondrial MnSOD genes *sod-1* and *sod-2*, respectively, *C. elegans* contains three additional isoforms: *sod-3*, a minor mitochondrial MnSOD; *sod-4* which is an extracellular Cu/ZnSOD responsible for up to 5% of all SOD activity in adult worms (Doonan *et al.*, 2008); and finally *sod-5*, a minor cytoplasmic SOD. A significant 10%–30% increase in oxidative damage for most strains was detected as compared with wild-type (Fig. 3C), suggesting that loss of SOD isoforms increases intrinsic oxidative damage. Interestingly, despite the small contribution of SOD-5 to total SOD activity and its expression limited to the ASI, ASK, and ADL neurons of *C. elegans* (Doonan *et al.*, 2008), a mutation of *sod-5* resulted in a dramatic increase in oxidative damage (Fig. 3C). This observation emphasizes the importance of oxidative damage defense and its critical regulation in these neurons. Moreover, whereas the *sod-1* mutant showed high sensitivity to PQ (Fig. 2D), no significant increase in oxidative damage was observed (Fig. 3C). Conversely, a mutant with extra *sod-1* copies [*wuIs152*(*sod-1* (genomic) + pRF4 (rol-6)] showed no decrease in oxidative damage (Fig. 3B). These findings suggest that the very high cytoplasmic SOD-1 levels are not required to protect against baseline ROS production, but rather protect the organism in specific conditions, such as in the harsh natural *C. elegans* environment.

To further address the sensitivity of our method, we tested a set of mitochondrial mutants, including *clk-1(qm30)* and *mev-1(kn1)* for which an altered ROS metabolism is expected. *clk-1* encodes for a ubiquinone biosynthetic enzyme (Van Raamsdonk & Hekimi, 2009) and mutant *clk-1(qm30)* is marked by a mild respiratory defect and extended lifespan (Van Raamsdonk & Hekimi, 2009). In contrast, *mev-1* encodes the succinate dehydrogenase cytochrome b and mutant *mev-1(kn1)* displays high sensitivity to PQ, decreased SOD activity and is short-lived (Adachi *et al.*, 1998). As shown in Fig. 3D, both *clk-1(qm30)* and *mev-1(kn1)* mutants showed increased oxidative damage as compared with N2 in line with their impaired electron transport function. Mutant *mev-1(kn1)* moreover showed a higher oxidative damage increase than *clk-1(qm30)* as compared with N2.

Finally, we tested if oxidative damage increased over age. As depicted in Fig. 3(E), an age-dependent increase in oxidative damage was found for both N2 and *sod-1* in conditions starting from the postreproductive phase (i.e., after day3/4 postdevelopment). Consistent with our findings, the *sod-1* mutant did not show increased oxidative damage levels as compared with N2 while aging (Fig. 3E, right panel).

Oxidative damage in longevity mutants

We next determined oxidative damage levels in a model for longevity by the highly conserved insulin/IGF-1 signaling pathway. In *C. elegans,* insulin signaling regulates metabolism, development, and longevity (Kenyon, 2010). Mutations in the homologue of the mammalian insulin receptor gene *daf-2*, arrest development in the dauer stage but weak or temperature sensitive mutations in *daf-2* can develop reproductively, but show increased energy storage and longevity (Kenyon, 2010). The lifespan extension caused by *daf-2* mutation is hypothesized to at least partially result from increased protection against stress, including oxidative stress (Lee *et al.*, 2003; Kenyon, 2010; Zarse *et al.*, 2012). Both the longevity and stress resistance response from the insulin/IGF-1 pathway requires the activity of the *daf-16* gene, which encodes a Forkhead transcription factor (Kenyon, 2010).

To determine oxidative damage in these longevity mutants, we analyzed the levels of F3-isoprostanes in young adults of *daf-2 (e1370)*, when the longevity pathway is active (Dillin *et al.*, 2002). As predicted by the Free radical theory of aging, we anticipated this mutant to have lower levels of oxidative damage. However, contrary to expectation, we found a more than 90% increase in oxidative

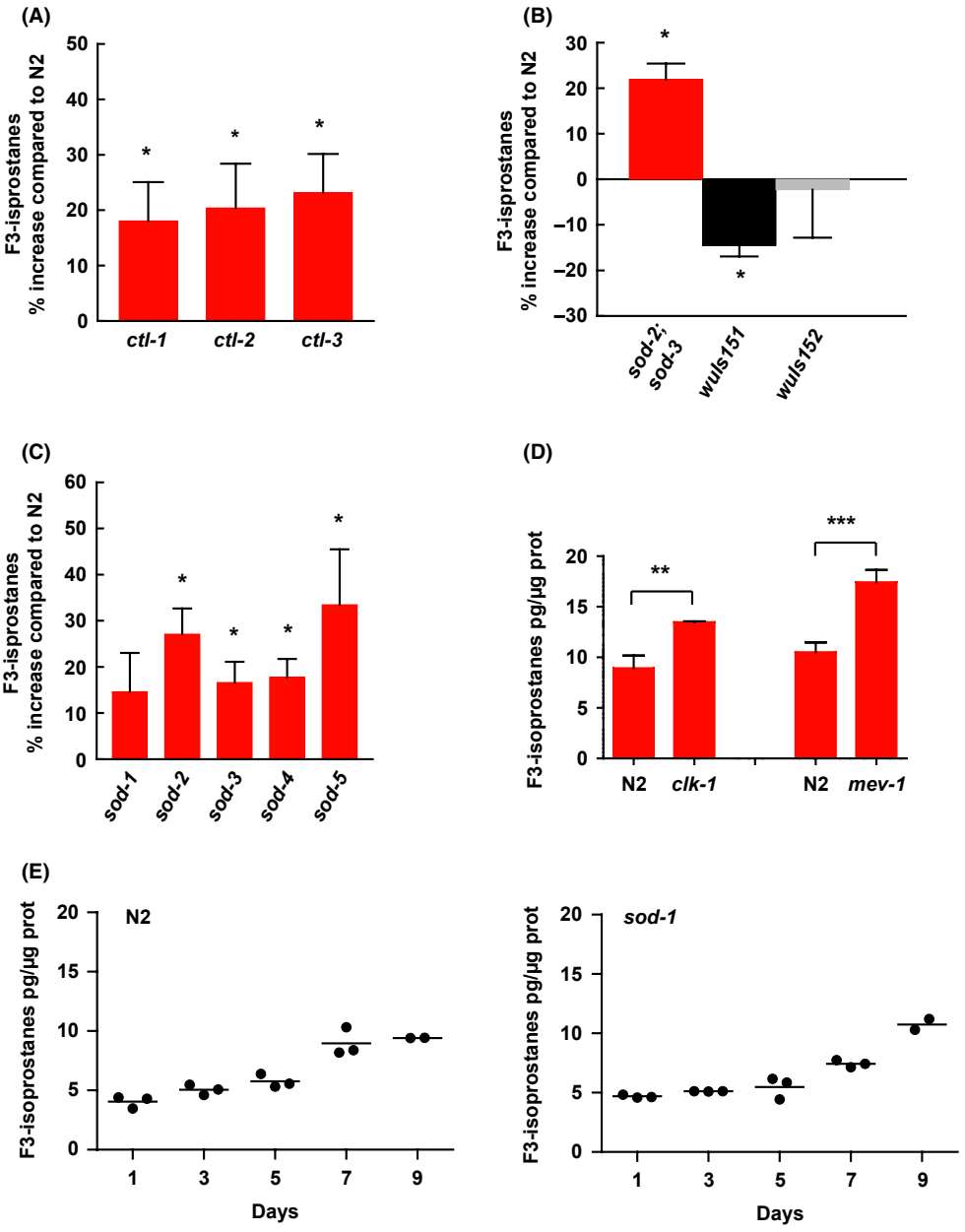

Fig. 3 F3-isoprostanes are increased in ROS-scavenging mutants, mitochondrial mutants, and aging worms. (A) Catalase (*ctl)* mutants showed increased F3-isoprostane levels compared with wild-type. The experiment was performed five times in triplicate and is shown as mean ± SEM (*$P < 0.05$). The significance of changes was confirmed by multiple comparisons testing of differences using Restricted Maximum Likelihood estimation (see Methods). (B) F3-isoprostane levels of ROS-scavenging mutant and transgenic worms. N2, *sod-2*(gk257); *sod-3*(tm760), *wuIs151* (*ctl-1* + *ctl-2* + *ctl-3* + *myo-2::GFP*), *wuIs152*[*sod-1* (genomic) + pRF4 (rol-6)], mutants were analyzed as in (A). The significance of changes was confirmed by Welch's *t*-test and are shown as mean ± SD (*$P < 0.05$). (C) An increase in F3-isoprostanes is measured in most SOD mutant strains. N2 plus *sod* mutants were analyzed as in (A). (D) The mitochondrial mutants *clk-1(qm30)* and *mev-1(kn1)* showed increased oxidative damage as compared with N2. Analysis was performed as in (A). The significance of changes was confirmed by Students *t*-test and are shown as mean ± SD (*$P < 0.05$). (E) Aging of *C. elegans* is associated with increasing F3-isoprostane levels. Synchronized populations of N2 (left panel) and *sod-1* (right panel) animals were analyzed at indicated ages as in (A). Scatter plots show individual data points with the mean indicated by the horizontal line.

damage in the long-lived *daf-2(e1370)* mutant which was partially suppressed in the *daf-16*(mu86)*; daf-2(e1370)* double mutant (Fig. 4A). Next, we determined the ROS damage levels of these mutants during aging, by synchronizing nematodes and harvesting them at various time points up to day 11 of adulthood (Fig. 4B). Oxidative damage of both N2 and the double-mutant *daf-16 (mu86)*; *daf-2(e1370)* increased during aging (Fig. 4C, 4E). Increased levels of oxidative damage were observed after reproductive age for N2 and *daf-16*(mu86); *daf-2*(e1370), the latter which furthermore showed a steep oxidative damage increase at day 8, just before most animals collapsed around their maximal lifespan (Fig. 4E). These findings suggest that oxidative damage increases with age. Interestingly, while *daf-2(e1370)* has much higher oxidative damage as young adult than the N2 or *daf-16 (mu86)*; *daf-2(e1370)* strain (Fig. 4A, D), levels rapidly decreased with age (Fig. 4D). However, at day 11, when about 75% of N2 and about 95% of *daf-2(e1370)* survived, age-matched levels of oxidative damage in *daf-2(e1370)* were significantly lower as compared with N2 (Fig. 4D). Thus, the young adulthood of the *daf-2* mutant is marked by an unexpected *daf-16*-dependent temporal phase of oxidative damage, whereas during postreproductive aging, the *daf-2(e1370)* has significantly less oxidative damage than the N2. Finally, we tested the mutant *age-1(hx546)*. *age-1* encodes a phosphoinositide-3 kinase which signals in the Insulin/IGF-1 pathway downstream of *daf-2* but upstream of *daf-16*. The mutant *age-1(hx546)* also extends lifespan in a *daf-16*-dependent manner albeit to a lesser extend as the *daf-2(e1370)* (Kenyon, 2010). Interestingly, at young adulthood *age-1(hx546)* did

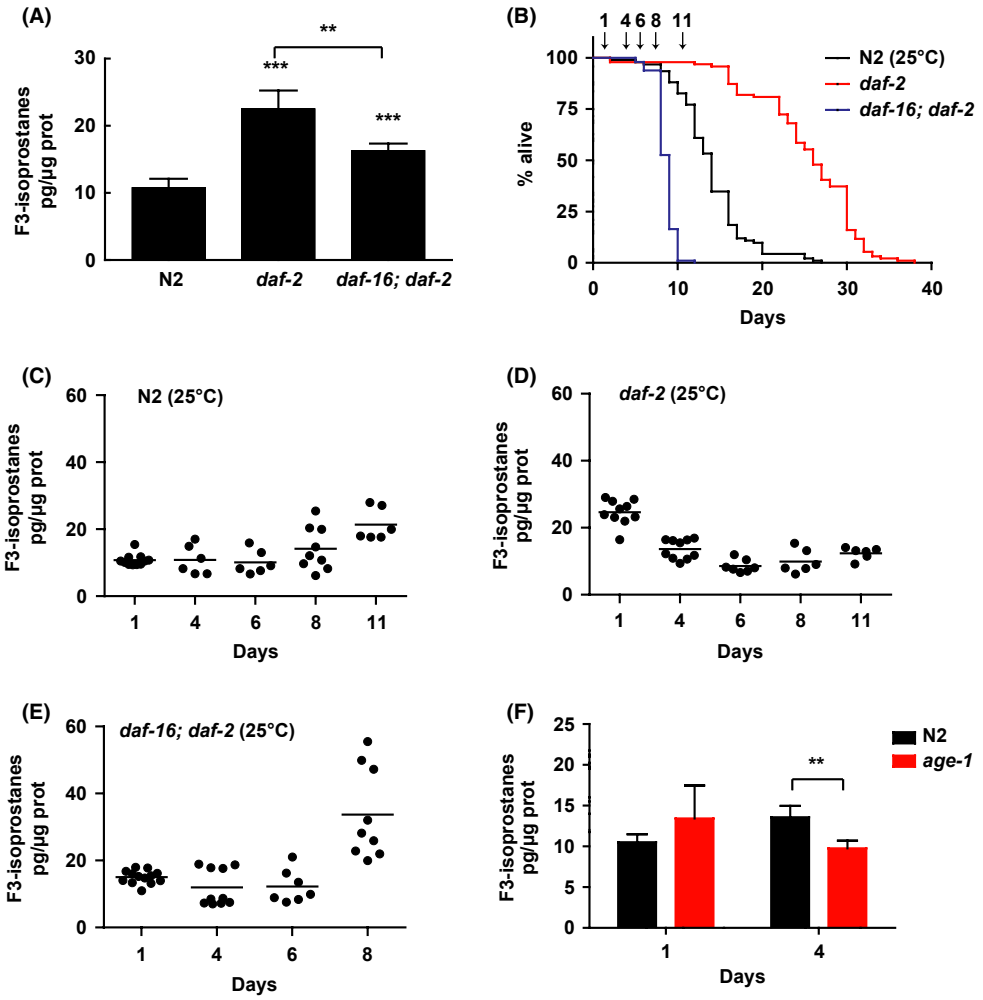

Fig. 4 Oxidative damage in Insulin/IGF-1 mutant during aging. (A) The *daf-2* mutant has increased levels of F3-isoprostanes relative to wild-type, partially rescued by *daf-16* at day 1 of adulthood. Young adult N2, *daf-2(e1370)* and *daf-16(mu86); daf-2 (e1370)* mutants were analyzed for F3-isoprostane levels. The experiments was performed three times in triplicate and is shown as mean ± SEM (*$P < 0.05$). (B) Lifespan curves of Insulin/IGF-1 mutants. All experiments were performed at least twice with >60 animals per condition. Arrows denote time of harvesting for analysis in (C–E). (C, D, E) Oxidative damage of N2 (C), *daf-2(e1370)* (D) and *daf-16(mu86); daf-2 (e1370)* mutants (E) during aging. The experiment was carried out as in (B) and animals were harvested at indicated time points. Scatter plots show individual data points with the mean indicated by the horizontal line. (F) N2 and *age-1(hx546)* mutants were analyzed for F3-isoprostane levels at indicated time points. The experiments was performed in sixfold and is shown as mean ± SD (*$P < 0.05$).

not show significantly increased oxidative damage, whereas at day 4 levels of oxidative damage were decreased as compared with N2 (Fig. 4F). These findings suggest that the temporal oxidative damage phase occurs upstream from *age-1*. Our findings furthermore indicate that oxidative damage levels of young adults do not necessarily reflect levels at older age, which highlights the need for longitudinal analysis to establish the role of oxidative damage during aging.

Discussion

Here, we describe the development of a robust, sensitive, and straightforward assay to quantify *in vivo* oxidative damage in *C. elegans* through LC-MS/MS-based quantification of endogenous F3-isoprostanes. These chemically stable products are produced by ROS-dependent lipid peroxidation of the predominant PUFA, EPA, in *C. elegans*. It is unlikely that F3-isoprostanes originated from the provided bacterial food source, *Escherichia Coli*, as *C. elegans* synthesizes EPA *de novo* by desaturation and elongation of saturated fatty acids from its bacterial food source (Watts & Browse, 2002). The formation of endogenous oxidative damage could be detected and quantified in whole animals, specifically in the cytoplasm or in organelles, such as mitochondria and peroxisomes. Moreover, even oxidative damage produced by only a few specific chemosensory neurons in the *C. elegans* head could be quantified, indicating high sensitivity and broad applicability of the method.

Several methods of oxidative damage quantification have been developed for *C. elegans* in the past but are generally accepted to lack sensitivity, specificity, or linearity (Muller *et al.*, 2007; Doonan *et al.*, 2008; Gems & Doonan, 2009). These have included application of fluorescent probes either in live animals or isolated mitochondria [e.g., 2′-7′-dichlorofluorescin (H_2DCF)] (Harding *et al.*, 2003; Schulz *et al.*, 2007). These methods suffer from methodological difficulties as it has been shown that these molecules can undergo photoreduction and produce reactive species (Marchesi *et al.*, 1999; Rota *et al.*, 1999). Fluorescent probes are prone to autofluorescence and require uptake by the animal or organelle or depend on promoter-driven expression, possibly introducing artifacts (e.g., distribution) and toxicity. These systems furthermore rely on optically accessible systems, which restrict their usage. Oxidative damage assessment in isolated mitochondria can also suffer from artifact introduction in the isolation process (Picard *et al.*, 2010). Finally, protein carbonylation is described as a marker for oxidative damage to proteins. This method relies on postlysis chemical

derivatization and antibody-based analysis. Linearity, specificity, and sensitivity are limited for this method and it could suffer from artificial carbonylation backgrounds introduced by oxygen, trace metals, and nucleic acids (Luo & Wehr, 2009). In contrast with these and other reported methods, F3-isoprostanes are produced endogenously and through the use of labeled internal standards and LC-MS/MS detection, they allow for detection with high specificity, sensitivity, and absolute quantification. Another distinguishing feature is that our method allowed thorough validation. Indeed, F3-isoprostane quantification is highly sensitive, detecting oxidative damage in less than 150 animals per sample, highly accurate, precise, and linear over a 2000-fold concentration range. In this respect, it is interesting to note that both *clk-1* and *mev-1* mutants showed increased oxidative damage levels. Although this finding is consistent with their phenotype of altered electron transport function (Adachi *et al.*, 1998; Van Raamsdonk & Hekimi, 2009), including decreased SOD activity, high PQ sensitivity, and strongly increased levels of protein carbonylation at older age for the *mev-1 (kn1)* (Ishii *et al.*, 2002), at young age both *clk-1(qm30)* and *mev-1 (kn1)* mutants did not show increased levels of protein carbonylation (Ishii *et al.*, 2002; Yang *et al.*, 2007). This finding could be explained by a higher sensitivity of F3- isoprostane analysis. However, further investigation will be required as these findings could additionally or alternatively reflect a difference in the type of quantified damage (lipid peroxidation vs. protein oxidation).

PQ has been proposed to induce superoxide radicals *in vivo* (Krall *et al.*, 1988) and time of survival in response to a lethal dose has often been used to determine oxidative damage resistance in *C. elegans*. We show that PQ-induced oxidative damage is indeed formed *in vivo*. In response to PQ, the *sod-1* mutant showed highest oxidative damage compared with wild-type and *sod-2*, suggesting that PQ induced oxidative damage predominantly in the cytoplasm. Consistent with its proposed mitochondrial localization, the *sod-2* mutant showed highest oxidative damage in response to the Complex I inhibitor rotenone. Surprisingly, in contrast with all other individual *sod* and *ctl* mutants, *sod-1*, which contributes to 80% of all of *C. elegans* SOD activity (Doonan *et al.*, 2008; Gems & Doonan, 2009), showed no significantly increased steady-state oxidative damage. This could be the consequence of functional redundancy by other ROS-scavenging enzymes. However, *sod-1* mutants showed extreme sensitivity to a high dose of PQ, in agreement with previous reports (Doonan *et al.*, 2008; Van Raamsdonk & Hekimi, 2009). Thus, these findings demonstrate that the resistance to induced oxidative damage phenotype does not automatically correlate with steady-state oxidative damage, underscoring the critical need for direct quantification of oxidative damage *in vivo*. Rather, we now propose that *sod-1* predominantly functions when challenged by adverse conditions, such as the harsh natural *C. elegans* environment. This notion is consistent with recent findings that a mutant which completely lacks SOD activity has normal lifespan yet high sensitivity to exogenous stressors (Van Raamsdonk & Hekimi, 2012). Interestingly, mutation of the second cytoplasmic SOD gene, *sod-5,* showed a 30% increase in oxidative damage. This is remarkable, given that its expression is predominantly localized to a small set of chemosensory neurons located in the nematode head and its expression contributes to less than 0.5% of all SOD mRNA (Doonan *et al.*, 2008). Further functional studies will be required to determine the consequences of these oxidative damage levels.

Using our method, we could for the first time accurately quantify oxidative damage of several nematode strains during aging. We note that nematodes increased oxidative damage levels with age and, as could be noted for the *daf-16(mu86)*; *daf-2(e1370)* double mutant, oxidative damage increased exponentially during aging being highest immediately before death of most nematodes. Surprisingly, the stress-resistant *daf-2(e1370)* insulin/IGF-1 receptor longevity mutant has a significantly higher level of oxidative damage at young adulthood than N2 wild-type nematodes and *daf-16 (mu86)*; *daf-2(e1370)* mutants. This is unexpected since *daf-2* mutants showed high resistance to a pro-oxidant challenge (Lee *et al.*, 2003) and, if oxidative damage would be the primary cause of aging, conflicts with its longevity phenotype. However, longitudinal analysis of synchronized aging *daf-2(e1370)* populations of nematodes revealed that this increased oxidative damage is temporarily, restricted to young adulthood and followed by a decrease in oxidative damage to levels that are significantly lower than the wild-type during postreproductive aging. These findings suggest that despite an initial period of high oxidative damage in young adulthood, impaired insulin/IGF-1 mutants accumulate less oxidative damage during postreproductive aging. Importantly, for all strains tested, oxidative damage was only found to increase during postreproductive aging. Thus, for the study of aging theories in *C. elegans*, we therefore propose to perform longitudinal analysis, rather than restricting to e.g., young adults only.

The longevity phenotype of lowered insulin/IGF-1 signaling is suppressed by *daf-16* (Kenyon, 2010) and we found that the temporal increase in oxidative damage in the *daf-2* mutant at least partially requires *daf-16*, suggesting that this oxidative damage phase contributes to its longevity phenotype. In this respect, it is interesting to note that the antioxidant N-acetyl-L-cysteine was found to decrease *daf-2* lifespan but not that of wild-type nematodes (Yang & Hekimi, 2010; Zarse *et al.*, 2012). In fact, our observations are consistent with the concept of mitohormesis which postulates that a temporal increase in ROS species originating from mitochondria triggers an adaptive cellular stress response of increased ROS defense and ultimately, an increased lifespan (Schulz *et al.*, 2007; Zarse *et al.*, 2012). Interestingly, whereas Zarse *et al.* showed increased hydrogen peroxide and mitochondrial ROS production after acute impairment of *daf-2* signaling by RNAi, we extend these observations by showing ROS damage in the constitutive impaired Insulin/IGF-1 signaling mutant *daf-2 (e1370)*. For insulin/IGF-1 signaling, this increase in ROS is thought to be triggered by a metabolic switch in response to decreased glucose levels as a consequence of impaired insulin/IGF-1 receptor function (Schulz *et al.*, 2007; Zarse *et al.*, 2012). Although further studies in *C. elegans* will be required to determine the contribution of oxidative damage to longevity, with respect to the concept of mitohormesis, our findings suggest that the transient ROS burst initiates early in adult life and importantly, is *daf-16* dependent, suggesting that the metabolic switch is governed by this

transcription factor. The transient increase in ROS is likely blunted later in life through increased expression of antioxidant genes, including SODs, catalases, glutathione S-transferases, and thioredoxins, in response to this ROS peak. Indeed, *daf-16* regulates gene expression of antioxidant genes, including SODs, catalases, glutathione S-transferases, and thioredoxins (Murphy *et al.*, 2003) and is activated by oxidative stress (Essers *et al.*, 2004).

In conclusion, we characterize a novel ultrasensitive approach to quantify *in vivo* endogenous oxidative damage in *C. elegans*. Our method follows a short protocol that employs Triple-Quadruple MS technology, readily available in most metabolomics, proteomics, and pharmacology laboratories. This method can easily be scaled up for screening purposes and applied to other model organisms. We anticipate that this method could prove useful toward understanding the contribution of ROS and oxidative damage in pathologies and the biology of aging.

Experimental procedures

Reagents

Synthetic 5-epi-8,12-iso-iPF$_{3\alpha}$-VI, 8,12-iso-iPF$_{3\alpha}$-VI, d4-5-epi-8,12-iso-iPF$_{3\alpha}$-VI and d4-8,12-iso-iPF$_{3\alpha}$-VI were synthesized as previously described(Chang *et al.*, 2008). Stock solutions were prepared in 100% ethanol and stored at −20°C. Chemicals used included Butylated hydroxytolueen (BHT), Trolox and Glucose Oxidase (Sigma Aldrich), Paraquat (Acros organics), and Rotenone (Fluka).

Caenorhabditis elegans strains and growth conditions

sod-1(tm776), *sod-2(gk257)*, *sod-3(tm760)*, *sod-4(gk101)*, *sod-5 (tm1146)*, *sod-2(gk257);sod-3(tm760)*, *wuIs151*(*ctl-1* + *ctl-2* + *ctl-3* + *myo-2*::*GFP*), *wuIs152*[*sod-1* (genomic) + *pRF4 (rol-6*)] were prepared by the Gems laboratory (Doonan *et al.*, 2008). These strains plus N2 (wild-type) and *ctl-1(ok1242) ctl-3(ok2042)*, *ctl-2 (ok1137)*, *daf-2(e1370)*, *daf-16(mu86)*; *daf-2(e1370)*, *age-1(hx546)*, *mev-1(kn1)*, and *clk-1(qm30)* were all obtained from *Caenorhabditis* Genetics Center (CGC, Minneapolis, USA). Strains were cultured on nematode growth media (NGM) agar at 20°C, containing *Escherichia coli* strain OP50 as food source. Worms were synchronized by bleaching to collect eggs as previously described (Dillin *et al.*, 2002). During longitudinal analysis nematodes were placed on fresh plates after 4 days. Unless otherwise stated, all worms were collected at day 1 of adulthood.

Lifespan analysis

Lifespan analysis was performed as described previously (Dillin *et al.*, 2002). In brief, synchronized nematodes were grown until L4, when transferred to fresh plates supplemented with 100 μM 2′fluoro-5′ deoxyuridine (FUDR; Sigma, St Louis, MO, USA). The prefertile period of adulthood was chosen as $T = 0$ for lifespan analysis. Strains were grown for at least two generations before lifespan analysis was started. Lifespan analysis of Insulin/IGF-1 mutants was conducted at 25°C. An animal was scored dead when it no longer responded to (mechanical) stimulation. Animals that ruptured, bagged, or crawled off the plates were censored. The first two phenomena occurred on few occasions. Statistical significance was calculated using the log-rank (Mantel-Cox) method.

Sample preparation and LC-MS/MS analysis

Detailed methods for the sample preparation and LC-MS/MS experiments are found in the method description of the Supplementary Information.

In vitro peroxidation of EPA and *C. elegans* homogenates

Eicosapentaenoyl PAF-C16 (Cayman Chemicals) was stored as a 5-mM stock solution in 100% ethanol under nitrogen at −20°C to ensure minimal auto-oxidation. For analysis, EPA PAF-C16 was diluted to 5 μM in PBS.

Pro-oxidant treatment of *C. elegans*

Assays were performed either on plate or in liquid solution. For in liquid solution assays, worms were placed into 12-well plates containing 2 ml of either PQ (50 or 200 mM), rotenone (5 or 50 μM), glucose oxidase (50 mU), or glucose (4.5 g/L) dissolved in M9 buffer. After treatment, worms were washed three times with M9 buffer and analyzed. Parallel cultures were used to assay survival. Death was scored when worms failed to respond to mechanical stimulation. For on plate assays, pro- and antioxidants were added to NGM at indicated concentrations, casted into plates and dried in the dark. A fresh OP50 lawn was seeded on plates and allowed to grow overnight where after nematodes were placed on for indicated times.

Quantification and statistical analysis

All data were normalized to the amount of protein per sample, using Bradford (BioRad) analysis. Experiments were done in triplicate (unless stated otherwise). Welch's *t*-test was used to test for significant differences between groups at $P < 0.05$ taking into account unequal variance. In case of equal variance, a Student's *t*-test was performed. For experiments with multiple comparisons of differences between mutants and N2, Restricted Maximum Likelihood (REML) estimation was performed, taking the random variation between experiments into account. The Wald test was used to assess significance of fixed effects; subsequent pairwise comparison of single mutants with N2 was performed using the least significance difference at $P < 0.05$.

Acknowledgments

A.B.B was cofinanced and E.C.S and C.L. were financed by grants from the Netherlands Metabolomics Centre which is part of the Netherlands Genomics Initiative / Netherlands Organisation for Scientific Research. We thank Tobias Dansen and Boudewijn Burgering and members of the Brenkman lab for stimulating

discussion and critical reading of the manuscript. The *Caenorhabditis* Genetic Center (University of Minnesota, Minneapolis) is acknowledged for providing nematode strains.

References

Adachi H, Fujiwara Y, Ishii N (1998) Effects of oxygen on protein carbonyl and aging in Caenorhabditis elegans mutants with long (age-1) and short (mev-1) life spans. *J. Gerontol. Series A, Biol. Sci. Med. Sci.* **53**, B240–244.

Albrecht SC, Barata AG, Grosshans J, Teleman AA, Dick TP (2011) In vivo mapping of hydrogen peroxide and oxidized glutathione reveals chemical and regional specificity of redox homeostasis. *Cell Metab.* **14**, 819–829.

Back P, De Vos WH, Depuydt GG, Matthijssens F, Vanfleteren JR, Braeckman BP (2012) Exploring real-time in vivo redox biology of developing and aging Caenorhabditis elegans. *Free Radic. Biol. Med.* **52**, 850–859.

Chamulitrat W, Mason RP (1989) Lipid peroxyl radical intermediates in the peroxidation of polyunsaturated fatty acids by lipoxygenase. Direct electron spin resonance investigations. *J. Biol. Chem.* **264**, 20968–20973.

Chang CT, Patel P, Kang N, Lawson JA, Song WL, Powell WS, FitzGerald GA, Rokach J (2008) Eicosapentaenoic-acid-derived isoprostanes: synthesis and discovery of two major isoprostanes. *Bioorg. Med. Chem. Lett.* **18**, 5523–5527.

Cocheme HM, Quin C, McQuaker SJ, Cabreiro F, Logan A, Prime TA, Abakumova I, Patel JV, Fearnley IM, James AM, Porteous CM, Smith RA, Saeed S, Carre JE, Singer M, Gems D, Hartley RC, Partridge L, Murphy MP (2011) Measurement of H2O2 within living Drosophila during aging using a ratiometric mass spectrometry probe targeted to the mitochondrial matrix. *Cell Metab.* **13**, 340–350.

Dillin A, Crawford DK, Kenyon C (2002) Timing requirements for insulin/IGF-1 signaling in C. elegans. *Science* **298**, 830–834.

Doonan R, McElwee JJ, Matthijssens F, Walker GA, Houthoofd K, Back P, Matscheski A, Vanfleteren JR, Gems D (2008) Against the oxidative damage theory of aging: superoxide dismutases protect against oxidative stress but have little or no effect on life span in Caenorhabditis elegans. *Genes Dev.* **22**, 3236–3241.

Essers MA, Weijzen S, De Vries-Smits AM, Saarloos I, De Ruiter ND, Bos JL, Burgering BM (2004) FOXO transcription factor activation by oxidative stress mediated by the small GTPase Ral and JNK. *The EMBO Journal.* **23**, 4802–4812.

Gao L, Yin H, Milne GL, Porter NA, Morrow JD (2006) Formation of F-ring isoprostane-like compounds (F3-isoprostanes) in vivo from eicosapentaenoic acid. *J. Biol. Chem.* **281**, 14092–14099.

Gems D, Doonan R (2009) Antioxidant defense and aging in C. elegans: is the oxidative damage theory of aging wrong? *Cell Cycle* **8**, 1681–1687.

Halliwell B (1999) Antioxidant defence mechanisms: from the beginning to the end (of the beginning). *Free Radic. Res.* **31**, 261–272.

Harding HP, Zhang Y, Zeng H, Novoa I, Lu PD, Calfon M, Sadri N, Yun C, Popko B, Paules R, Stojdl DF, Bell JC, Hettmann T, Leiden JM, Ron D (2003) An integrated stress response regulates amino acid metabolism and resistance to oxidative stress. *Mol. Cell* **11**, 619–633.

Harman D (1956) Aging: a theory based on free radical and radiation chemistry. *J. Gerontol.* **11**, 298–300.

Hunter T, Bannister WH, Hunter GJ (1997) Cloning, expression, and characterization of two manganese superoxide dismutases from Caenorhabditis elegans. *J. Biol. Chem.* **272**, 28652–28659.

Ishii N, Goto S, Hartman PS (2002) Protein oxidation during aging of the nematode Caenorhabditis elegans. *Free Radic. Biol. Med.* **33**, 1021–1025.

Kadiiska MB, Gladen BC, Baird DD, Germolec D, Graham LB, Parker CE, Nyska A, Wachsman JT, Ames BN, Basu S, Brot N, Fitzgerald GA, Floyd RA, George M, Heinecke JW, Hatch GE, Hensley K, Lawson JA, Marnett LJ, Morrow JD, Murray DM, Plastaras J, Roberts LJ 2nd, Rokach J, Shigenaga MK, Sohal RS, Sun J, Tice RR, Van Thiel DH, Wellner D, Walter PB, Tomer KB, Mason RP, Barrett JC (2005) Biomarkers of oxidative stress study II: are oxidation products of lipids, proteins, and DNA markers of CCl4 poisoning? *Free Radic Biol Med.* **38**, 698–710.

Kenyon CJ (2010) The genetics of ageing. *Nature* **464**, 504–512.

Krall J, Bagley AC, Mullenbach GT, Hallewell RA, Lynch RE (1988) Superoxide mediates the toxicity of paraquat for cultured mammalian cells. *J. Biol. Chem.* **263**, 1910–1914.

Lee SS, Kennedy S, Tolonen AC, Ruvkun G (2003) DAF-16 target genes that control C. elegans life-span and metabolism. *Science* **300**, 644–647.

Li N, Ragheb K, Lawler G, Sturgis J, Rajwa B, Melendez JA, Robinson JP (2003) Mitochondrial complex I inhibitor rotenone induces apoptosis through enhancing mitochondrial reactive oxygen species production. *J. Biol. Chem.* **278**, 8516–8525.

Luo S, Wehr NB (2009) Protein carbonylation: avoiding pitfalls in the 2,4-dinitrophenylhydrazine assay. *Redox Rep.* **14**, 159–166.

Maiorino M, Zamburlini A, Roveri A, Ursini F (1995) Copper-induced lipid peroxidation in liposomes, micelles, and LDL: which is the role of vitamin E? *Free Radic. Biol. Med.* **18**, 67–74.

Marchesi E, Rota C, Fann YC, Chignell CF, Mason RP (1999) Photoreduction of the fluorescent dye 2′-7′-dichlorofluorescein: a spin trapping and direct electron spin resonance study with implications for oxidative stress measurements. *Free Radic. Biol. Med.* **26**, 148–161.

Morrow JD, Hill KE, Burk RF, Nammour TM, Badr KF, Roberts LJ 2nd (1990) A series of prostaglandin F2-like compounds are produced in vivo in humans by a non-cyclooxygenase, free radical-catalyzed mechanism. *Proc. Natl. Acad. Sci. U S A.* **87**, 9383–9387.

Muller FL, Lustgarten MS, Jang Y, Richardson A, Van Remmen H (2007) Trends in oxidative aging theories. *Free Radic. Biol. Med.* **43**, 477–503.

Murphy CT, McCarroll SA, Bargmann CI, Fraser A, Kamath RS, Ahringer J, Li H, Kenyon C (2003) Genes that act downstream of DAF-16 to influence the lifespan of Caenorhabditis elegans. *Nature* **424**, 277–283.

Paraidathathu T, De Groot H, Kehrer JP (1992) Production of reactive oxygen by mitochondria from normoxic and hypoxic rat heart tissue. *Free Radic. Biol. Med.* **13**, 289–297.

Picard M, Ritchie D, Wright KJ, Romestaing C, Thomas MM, Rowan SL, Taivassalo T, Hepple RT (2010) Mitochondrial functional impairment with aging is exaggerated in isolated mitochondria compared to permeabilized myofibers. *Aging Cell* **9**, 1032–1046.

Pratico D, Tangirala RK, Rader DJ, Rokach J, FitzGerald GA (1998) Vitamin E suppresses isoprostane generation in vivo and reduces atherosclerosis in ApoE-deficient mice. *Nat. Med.* **4**, 1189–1192.

Pratico D, Rokach J, Lawson J, FitzGerald GA (2004) F2-isoprostanes as indices of lipid peroxidation in inflammatory diseases. *Chem. Phys. Lipids* **128**, 165–171.

Rokach J, Khanapure SP, Hwang SW, Adiyaman M, Lawson JA, FitzGerald GA (1997) Nomenclature of isoprostanes: a proposal. *Prostaglandins* **54**, 853–873.

Rota C, Chignell CF, Mason RP (1999) Evidence for free radical formation during the oxidation of 2′-7′-dichlorofluorescin to the fluorescent dye 2′-7′-dichlorofluorescein by horseradish peroxidase: possible implications for oxidative stress measurements. *Free Radic. Biol. Med.* **27**, 873–881.

Schulz TJ, Zarse K, Voigt A, Urban N, Birringer M, Ristow M (2007) Glucose restriction extends Caenorhabditis elegans life span by inducing mitochondrial respiration and increasing oxidative stress. *Cell Metab.* **6**, 280–293.

Song WL, Paschos G, Fries S, Reilly MP, Yu Y, Rokach J, Chang CT, Patel P, Lawson JA, Fitzgerald GA (2009) Novel eicosapentaenoic acid-derived F3-isoprostanes as biomarkers of lipid peroxidation. *J. Biol. Chem.* **284**, 23636–23643.

Taber DF, Morrow JD, Roberts LJ 2nd (1997) A nomenclature system for the isoprostanes. *Prostaglandins* **53**, 63–67.

Van Raamsdonk JM, Hekimi S (2009) Deletion of the mitochondrial superoxide dismutase sod-2 extends lifespan in Caenorhabditis elegans. *PLoS Genet.* **5**, e1000361.

Van Raamsdonk JM, Hekimi S (2012) Superoxide dismutase is dispensable for normal animal lifespan. *Proc. Natl Acad. Sci. USA* **109**, 5785–5790.

Van Raamsdonk JM, Meng Y, Camp D, Yang W, Jia X, Benard C, Hekimi S (2010) Decreased energy metabolism extends life span in Caenorhabditis elegans without reducing oxidative damage. *Genetics* **185**, 559–571.

Watts JL, Browse J (2002) Genetic dissection of polyunsaturated fatty acid synthesis in Caenorhabditis elegans. *Proc. Natl Acad. Sci. USA* **99**, 5854–5859.

Yang W, Hekimi S (2010) A mitochondrial superoxide signal triggers increased longevity in Caenorhabditis elegans. *PLoS Biol.* **8**, e1000556.

Yang W, Li J, Hekimi S (2007) A Measurable increase in oxidative damage due to reduction in superoxide detoxification fails to shorten the life span of long-lived mitochondrial mutants of Caenorhabditis elegans. *Genetics* **177**, 2063–2074.

Zarse K, Schmeisser S, Groth M, Priebe S, Beuster G, Kuhlow D, Guthke R, Platzer M, Kahn CR, Ristow M (2012) Impaired insulin/IGF1 signaling extends life span by promoting Mitochondrial L-Proline Catabolism to induce a transient ROS signal. *Cell Metab.* **15**, 451–465.

Supporting Information

Additional Supporting Information may be found in the online version of this article at the publisher's web-site.

Fig. S1 Identification of two F3-isoprostane isomers in *C. elegans*

Fig. S2 Method description

Table S1 Method accuracy and precision of F3-isoprostane quantification